

Creep and Creep-Fatigue Crack Growth in Aluminium Alloys

Gilbert Hénaff¹, Grégory Odemer² and Bertrand Journet³

¹*Institut Pprime, UPR 3346 CNRS – ENSMA – Université de Poitiers*

²*Cirimat, Ensiacet, Toulouse*

³*EADS IW, Suresnes
France*

1. Introduction

Due to the low melting point of aluminium and its consequences on microstructural stability and mechanical resistance, aluminium alloys are generally not considered for applications that have to withstand elevated temperatures in service. However, in some very specific instances where the temperature is not too high, aluminium alloys can present a unique solution. In addition, for such applications, the damage tolerance assessment can be a key issue and data as well as predictive models of propagation life are needed to meet the requirements. This is the case for fuselage panels for civil transport aircraft: a cruise speed of Mach 2.05 induces a maximum temperature of the fuselage skin of 130°C. Concorde, the first supersonic civil transport aircraft, was originally designed to sustain 7000 flights, i.e. 15000 hours. The fuselage design was conducted by considering creep deformation of the 2618A aluminium alloy used for fuselage skin on one hand, and the fatigue resistance of this alloy on the other hand. However, as the damage tolerance philosophy was not mature at that time, life predictions were mainly based on safe life concepts, without specific consideration of crack growth. More recently, a future supersonic aircraft was designed to sustain a total of 20000 flights, i.e. 60000 hours at almost the same elevated temperature (130°C). In this design the fuselage skin was still be made of aluminium alloy. In addition, this structure had to meet damage tolerance requirements, which requires reliable fatigue crack growth models. Such models should account for the physical mechanisms that affect crack growth at elevated temperature, including creep damage. However, issues related to creep-fatigue interactions during crack growth have not been extensively studied so far in aluminium alloys. One can however find some information in (Kaufman et al., 1976; Bensussan et al., 1984; Bensussan et al., 1988; Jata et al., 1994). With this respect, the present chapter presents an overview of the creep crack growth and creep-fatigue crack growth resistance of a precipitation-hardened aluminium 2650 T6 alloy, which is precisely the alloy selected for this type of application. More precisely, it reports on investigations that have been carried out to identify the mechanisms that would control possible creep-fatigue interactions in the 2650 T6 aluminium alloy and to evaluate the conservatism of the cumulative damage rule. With this aim, crack growth data have been established not only under creep-fatigue loading, but also under fatigue and creep loading. Most of the tests were carried out in the 100-175°C temperature range in laboratory air. Some additional tests were carried out in

vacuum in order to evaluate the effect of environment on these processes. The Creep Crack Growth (CCG) behaviour of the 2650 T6 aluminium alloy is first presented. Similarly, the Fatigue Crack Growth (FCG) behaviour is examined at room temperature and elevated temperatures. Finally, the Creep-Fatigue Crack Growth (CFCG) is studied by means of low frequency signals with different waveshapes. The analysis of creep-fatigue mechanisms is supported by quantitative fracture surface observations by scanning electron microscopy. Finally the ability of simple cumulative rules to correctly account for the CFCG behaviour is examined and discussed.

2. Material and experimental techniques

2.1 Material

The 2650 alloy is a copper-magnesium aluminium alloy, provided in the form of sheets (thickness: 2.5 and 5mm). The chemical composition is given in Table 1.

Analysis	Si	Fe	Cu	Mn	Mg	Cr	Ni	Zn	Ti	Zr
Min	0.36	0.08	2.60	0.32	1.50				0.08	
Expected	0.40	0.11	2.70	0.35	1.60				0.10	
Max	0.44	0.13	2.80	0.38	1.70	0.04	0.03	0.10	0.12	0.03

Table 1. Chemical composition of the 2650 aluminium alloy.

T(°C)	σ_Y (MPa) L	σ_Y (MPa) LT
20°C	421	411
100°C	394	386
130°C	375	371

Table 2. Yield strength σ_Y as a function of temperature for two orientations (data from EADS IW).

The CCG, FCG and CFCG resistance of this alloy is investigated after T6 artificial ageing treatment (192°C for 21 hours) resulting into a fully recrystallised microstructure with an average grain size of 40 μ m in the rolling plane. The precipitation hardening of this alloy has been studied by Majimel et al. (Majimel et al., 2002; Majimel et al., 2002). For this composition, the precipitation hardening system is Al-S (Al_2CuMg). Besides, results of hardness and tensile tests carried out on specimens aged 20000 hours at 175°C and 30000 hours at 100°C and 130°C respectively have shown no significant decay in mechanical properties with respect to those measured without prior ageing treatment, suggesting that bulk ageing effects during long-time crack growth experiments at elevated temperatures can be neglected (Odemer, 2005).

2.2 Testing

CCG, FCG and CFCG testing were performed on CT specimens ($W=32$ mm) of 5 mm thickness in the L-T orientation. The crack length was monitored by means of the potential

drop technique for the three types of test. For CCG tests, the samples were precracked by fatigue at room temperature. The initial value of K at the beginning of the creep test was higher than the value of K_{max} achieved at the end of the fatigue precracking in order to avoid a possible interaction between the fatigue precracking zone and the creep zone. CCG tests were carried out using dead-weight lever-type creep machines to apply a constant load. FCG and CFCG were conducted under a constant load ratio $R=0.5$ on a servohydraulic machine equipped with a furnace. The same load ratio was used during tests in vacuum. These tests were carried out on a servo-hydraulic machine equipped with a furnace and a chamber operating at a residual pressure of about 10^{-7} mbar. Crack closure measurements were performed by means of a capacitive displacement sensor. A triangular waveform loading with frequencies of 20Hz and 0.05Hz was used for fatigue tests. The 0.05Hz fatigue tests present the same loading increase/decrease times (10s) that trapezoidal waveform loading tests applied for creep-fatigue conditions and different hold-time durations (30, 300, 1500 and 3000 seconds) have been considered for CFCG tests.

3. Crack growth results and analysis

3.1 Creep crack growth

First, it is worth noticing that during CCG experiments, crack extension was not detected immediately after application of the load. The time during which no crack advance is measured is called incubation time and noticed t_i . Its value was experimentally determined as the time required to obtain a 1mV variation in the potential drop, as proposed by Bensussan (Bensussan et al., 1988), which corresponds to a crack advance of about 0,05mm. The t_i values obtained at different loads at 130°C are given in the table 2. This time can be interpreted as the time necessary to accumulate a critical amount of creep damage at the precrack tip to initiate propagation. According to Vitek (Vitek, 1977) this crack initiation would be governed by a critical value of the crack opening displacement. Ewing (Ewing, 1978) and Riedel (Riedel, 1977) using a modified Dugdale model, suggest that at high stresses: $t_i \propto K_i^{-2n}$, where n is the creep power law exponent. However the data obtained in the present study obey to the following law: $t_i \propto K_i^{-2}$, which means that the n exponent value is different from that derived from creep experiments. This discrepancy between theory and experimental results may be partly accounted for by the fact that the experimental incubation time may also include a propagation stage where the CCG rate is so slow that it cannot be detected by the potential drop method (Bensussan, Maas et al., 1988).

Incubation time (h)	K-level (MPa x m ^{1/2})
192	20
96	29
72	33

Table 2. Incubation time as a function of the initial stress intensity factor K_i at 130°C.

The influence of temperature on the CCG resistance of the 2650 alloy is shown in Figure 1 . Three domains, schematically represented in Figure 2, can be distinguished on CCG curves, regardless of temperature:

- a first domain where, just after incubation, Creep Crack Growth Rates (CCGRs) rapidly increases with K values; it was shown that, for a given temperature, the behaviour in this domain is also affected by initial load level (Odemer et al., 2006).
- a domain, corresponding with intermediate K values, where, except at 100°C, CCGRs obeys a fourth power law dependence with respect to K ($\frac{da}{dt} \propto K^4$); it is interesting to note that a similar power-law is predicted by theoretical models (see (Sadananda, 1978; Vitek, 1978));
- finally a third domain, characterised by a pronounced CCGR enhancement, corresponds with K values close to the critical value for fracture.

The values of the exponents noticed in the stage II and stage III, as the K and $\frac{da}{dt}$ range concerned, are given in table 3.

T (°C)	[K ₂] (MPa × m ^{1/2})	[da/dt] ₂ (m/s)	β ₂	[K ₃] (MPa × m ^{1/2})	[da/dt] ₃ (m/s)	β ₃
100	29-47	5.10 ⁻¹⁰ -3.10 ⁻⁸	8,47	47-52	5.10 ⁻⁸ -3x10 ⁻⁷	22,36
130	22-35,5	10 ⁻⁹ -6.10 ⁻⁹	3,88	35,5-47,5	6.10 ⁻⁹ -1.10 ⁻⁷	10,17
160	16-31	2.10 ⁻⁹ -3.10 ⁻⁸	4,04	35-50	5.10 ⁻⁸ -10 ⁻⁶	8,33
175	19-42	2.10 ⁻⁸ -5.10 ⁻⁷	4,08	42-52	5.10 ⁻⁷ -2.10 ⁻⁶	8,03

Table 3. Values of the CCG power law exponents (cf. Figure 2) exponents in the steady state regime at different temperatures.

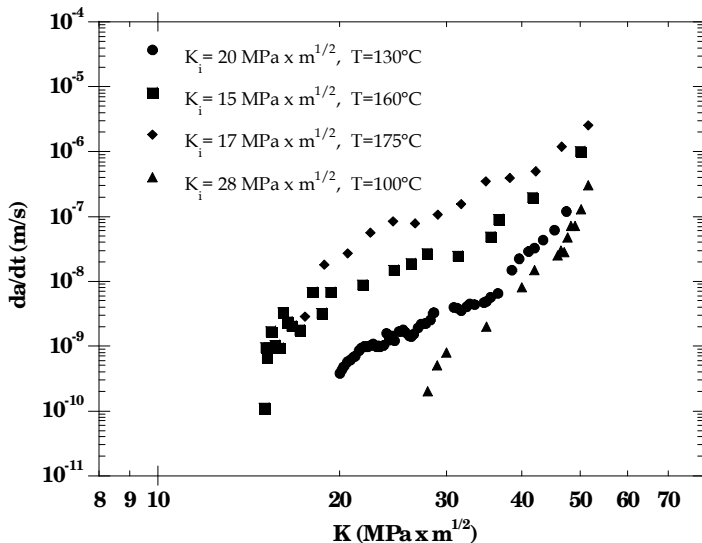


Fig. 1. Influence of temperature on CCG rates in the 2650 T6 alloy.

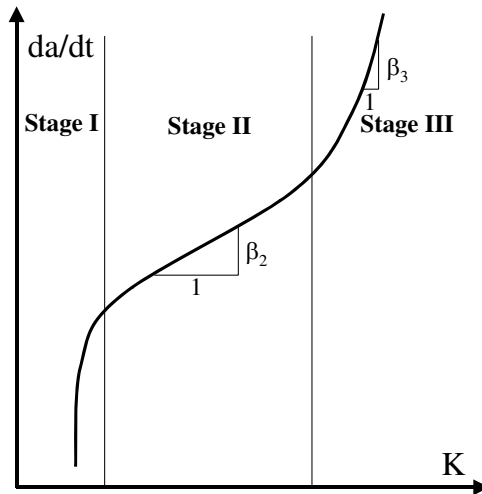


Fig. 2. Schematic representation of CCG curve.

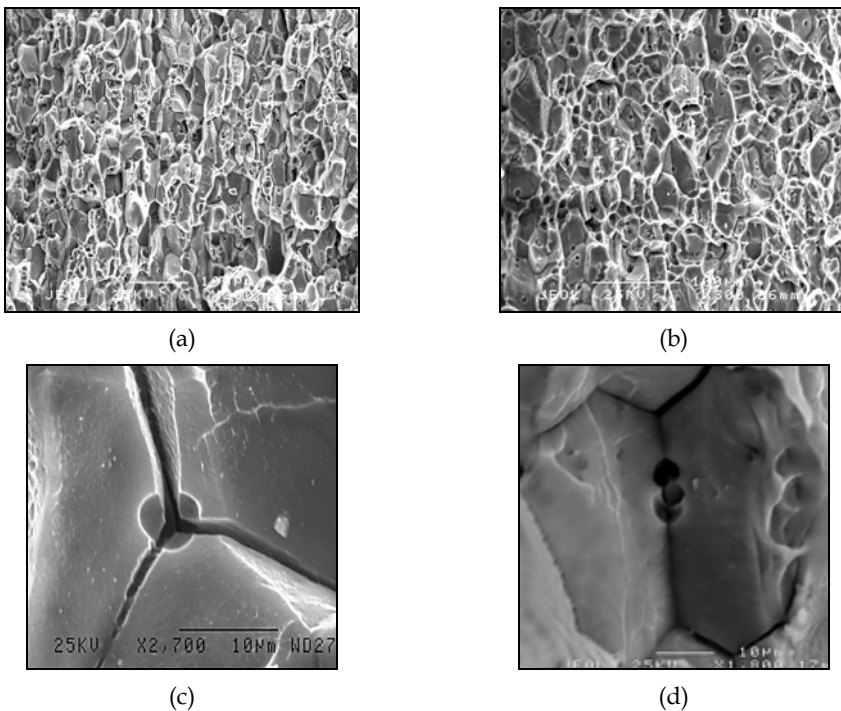


Fig. 3. Fracture surfaces produced during CCG (a) intergranular fracture ($K=22 \text{ MPa} \times \text{m}^{1/2}$, 175°C), (b) Intergranular and ductile rupture ($K=44 \text{ MPa} \times \text{m}^{1/2}$, 175°C); (c) Cavities nucleation at triple boundaries; (d) Coalescence of cavities.

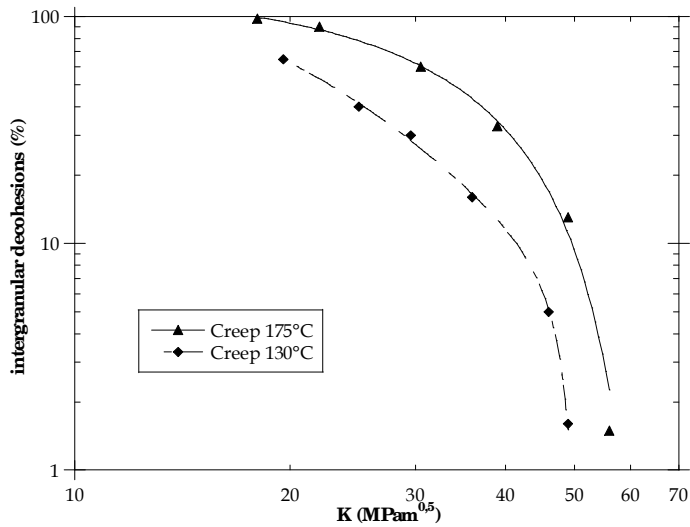


Fig. 4. Evolution of the intergranular decohesions during creep crack growth.

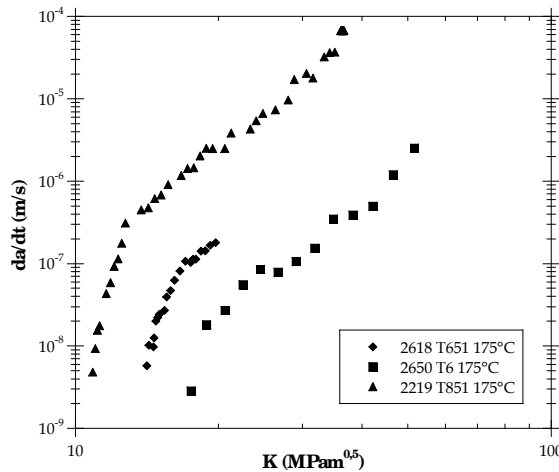


Fig. 7. Creep crack growth resistance of the 2650 T6, 2618 T651 (Leng, 1995) and 2219 T851 (Bensussan et al., 1984) alloys.

It can be seen that the CCG resistance is slightly affected by temperature in the range 100-130°C, except in the low K value domain. The temperature effect is more pronounced in the range 130-160°C and seems to saturate between 160°C and 175°C. This influence of temperature is consistent with results previously obtained on 2219 (Bensussan et al., 1984) and 2618 (Leng, 1995) alloys. However the second regime is larger at higher temperatures, although initial load may also account for this discrepancy. CCG fracture surfaces exhibit two characteristic failure modes, namely an intergranular fracture mode prevailing in the

slow growth rate regime (Figure 3 a) and a mixture of intergranular and ductile fractures which develops when approaching failure (Figure 3 b). The intergranular mode occurs by cavitation. The cavities nucleate at triple grain boundaries (Figure 3 c) or on precipitates along grain boundaries (Figure 3 d). This cavitation process is promoted at elevated temperature, as confirmed by quantitative measurements of the area percentage occupied by intergranular facets (Hénaff et al., 2010) presented in Figure 4.

The comparison presented in Figure 7 of the creep crack growth resistance of the 2650 T6 alloy and the resistance of 2618 T651 (Leng, 1995) and 2219 T851 (Bensussan et al., 1984) aluminium alloys at 175°C indicates a superior resistance of the 2650 T6 alloy, at least at his temperature. However an ageing effect cannot be excluded at this temperature (175°C) which is close to the heat-treatment temperature (192°C for 21h) of the 2650 alloy. However such an effect when exists would be beneficial to crack growth resistance.

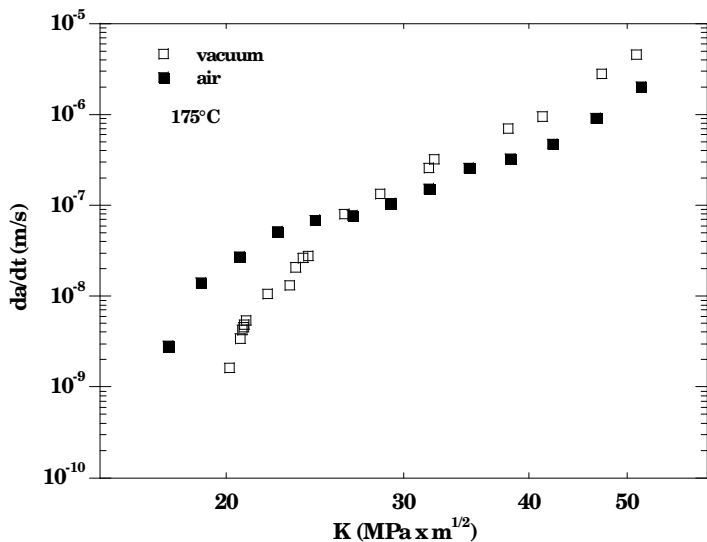


Fig. 5. CCG behaviour in air and in vacuum of the 2650 T6 alloy at 175°C.

In order to investigate possible environmental effects on crack growth, CCG rates obtained in air and in vacuum at 175°C are compared in Figure 5. It can be seen that CCG rates are nearly identical over the entire explored range. The difference noticed at low K values is difficult to analyse since it was shown that, for a given environment, the behaviour is influenced by initial load levels (Odemer et al., 2006). At high K values CCG rates in vacuum are slightly higher than those observed in air, as observed by Leng (Leng, 1995) on a 2618 alloy. However, apart from these small discrepancies, one can consider that the CCG resistance of the 2650 alloy is almost unaffected by environmental effects. However, as noticed by (Kaufman et al., 1976), this results demonstrates that stable crack growth under static load in air is not due to a stress corrosion cracking process which might also result into intergranular cracking (Menan and Hénaff, 2009).

3.2 Fatigue and Creep-fatigue crack growth

Figure 6 compares FCG rates measured at 20°C, 130°C and 175°C for load frequencies of 20Hz and 0.05Hz. At the load ratio considered, namely $R=0.5$, no crack closure effect was detected, regardless of temperature. Actually, even at $R=0.1$, crack closure effects are limited in this material (Odemer, 2005). It can be seen that temperature has almost no influence on FCG rates, and that frequency has only a slight influence on FCG rates in the 20-0.05Hz frequency range at 175°C. However, this slight deleterious effect is accompanied by a change in fracture surfaces, with a sharp increase in the surface fraction of intergranular decohesions similar to those observed during CCG, as shown in Figure 8. This effect, both on growth rates and fracture surfaces, suggests that, at low frequency, creep damage can occur during cyclic loading. In order to get further insights into this damage process occurring at elevated temperature, a hold time was introduced at the maximum load of the triangular loading. Figure 9 compares CFCG measured at 175°C for a 10s-0s-10s triangular loading and a 10s-300s-10s trapezoidal loading. A deleterious influence of hold-time on crack growth rates is noticed, more particularly in the $8 \text{ MPa} \times \text{m}^{1/2}$ - $40 \text{ MPa} \times \text{m}^{1/2}$ K_{\max} range. Therefore, different hold-time durations (0s, 30 s, 300s, and 1500s) have been considered in order to evaluate the creep damage effect as a function of hold-time only for loadings at $R=0.5$ (Odemer et al., 2006). The results obtained at 175°C are presented in Figure 10. It can be noticed that CFCG rates significantly increase as hold-time duration increases, indicating a significant contribution of creep damage to crack advance. A similar influence of hold time, although less pronounced, is also observed at 130°C. CFCG rates measured at 130°C and 175°C for the same hold-time duration, namely 300s, are compared in Figure 11. The hold time effect is more pronounced at 175°C, since it was shown that the FCG behaviour is only slightly affected by temperature (Figure 6).

A typical CFCG fracture surface is presented in Figure 12 a. The main observation is that, for a selected K value, CFCG fracture surfaces are not fundamentally different from those

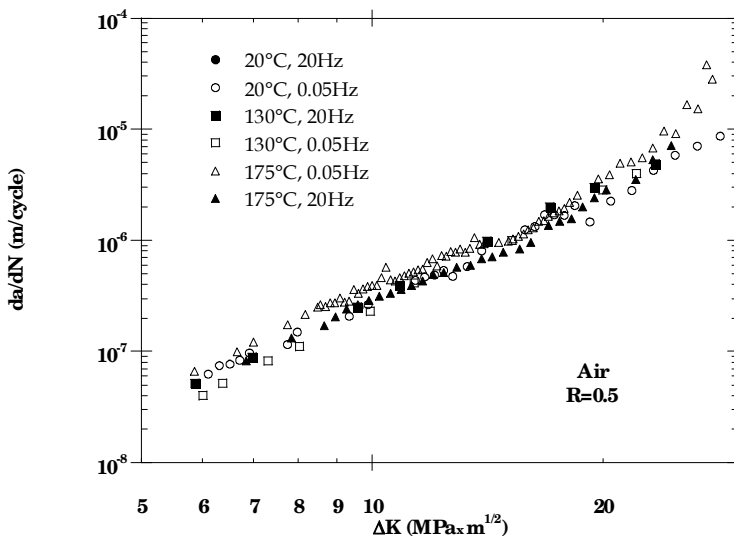


Fig. 6. Fatigue crack growth rates vs. ΔK at 20°C, 130°C and 175°C in air.

produced during FCG at 0.05Hz (10s-0s-10s). However the introduction of a hold-time at maximum load results into a higher percentage of intergranular decohesions. Additionally, as during CCG, the intergranular fracture seems to be controlled by cavitation (Figure 12 b). The same statement still holds at 130°C, although the amount of intergranular fracture is lower for a fixed loading condition. Additional testing using different waveshape signals (saw-tooth, triangle) indicate that it is the load period, and not the waveshape, that governs the crack growth enhancement during creep-fatigue, as shown in Figure 13. Indeed, CFCG rates obtained under saw-tooth signals, with a rapid or a slow loading rate, are identical to those obtained under trapezoidal waveshape with the same frequency. This suggests that there is no interaction between the additional damage process taking place at elevated temperature and the cyclic damage, conversely to what can be observed in corrosion-fatigue (Menan and Hénaff, 2009). With this respect, CFCG rates are plotted as a function of load period for selected values of K_{max} at $R=0.5$, at 130°C and 175°C in Figure 14a and Figure 14b respectively. The linear dependence in the right-hand part of these diagrams suggests that the time-dependent damage is governed by hold-time above a critical value of period T_c , which is dependent on temperature. Hence it is found that $T_c \approx 50s$ at 175°C, while $T_c \approx 320s$ at 130°C. A similar influence of frequency has been observed in 2219-T851 (Bensussan et al., 1984) and 8009 aluminium alloys (Jata et al., 1994).

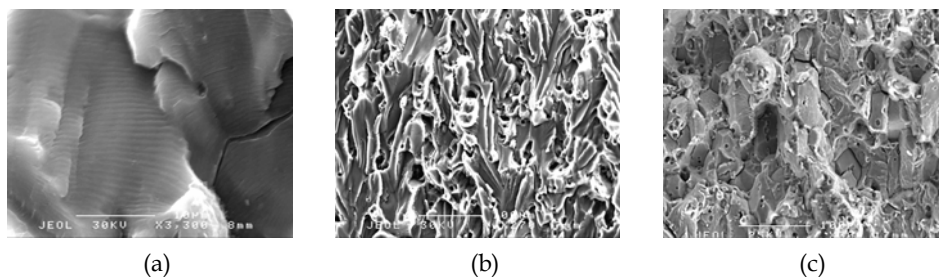


Fig. 7. Fracture surfaces produced during fatigue crack growth in the 2650 T6 alloy (a) at $\Delta K=9 \text{ MPa} \times \text{m}^{1/2}$, 20°C, 20 Hz, (b) at $\Delta K=9 \text{ MPa} \times \text{m}^{1/2}$, 130°C, 20 Hz and (c) at $\Delta K=7 \text{ MPa} \times \text{m}^{1/2}$, 175°C, 0.05Hz.

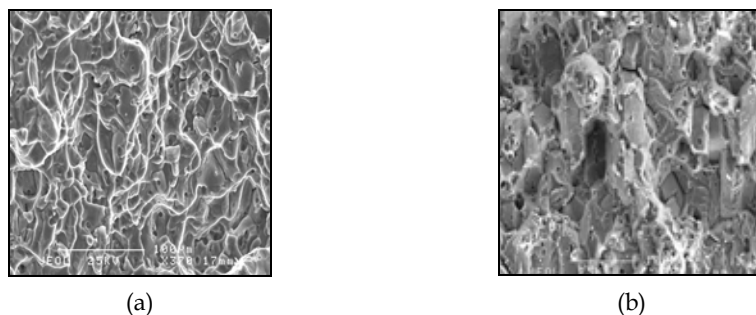


Fig. 8. Fractures surfaces obtained at 0.05Hz (a) 130°C, $da/dN=1 \times 10^{-7} \text{ m/cycle}$, (b) 175°C, $da/dN=1 \times 10^{-7} \text{ m/cycle}$.

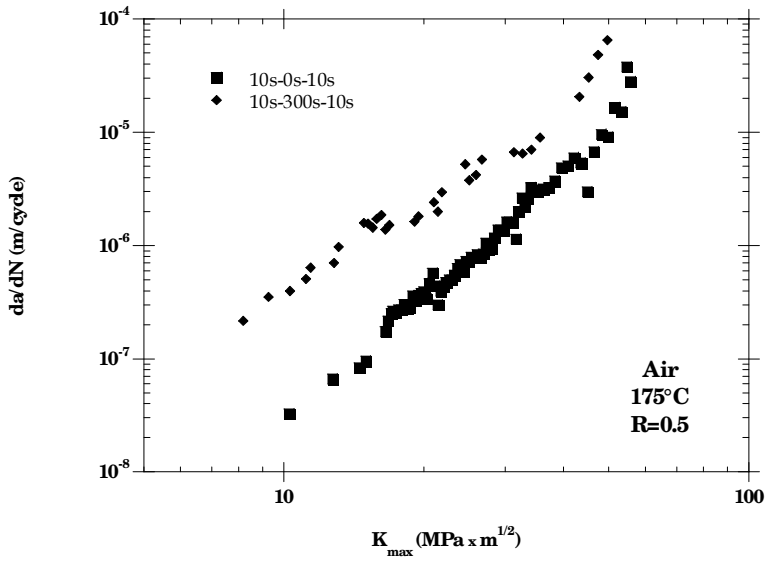


Fig. 9. FCG and CFCG rates vs. K_{max} (175°C) in air.

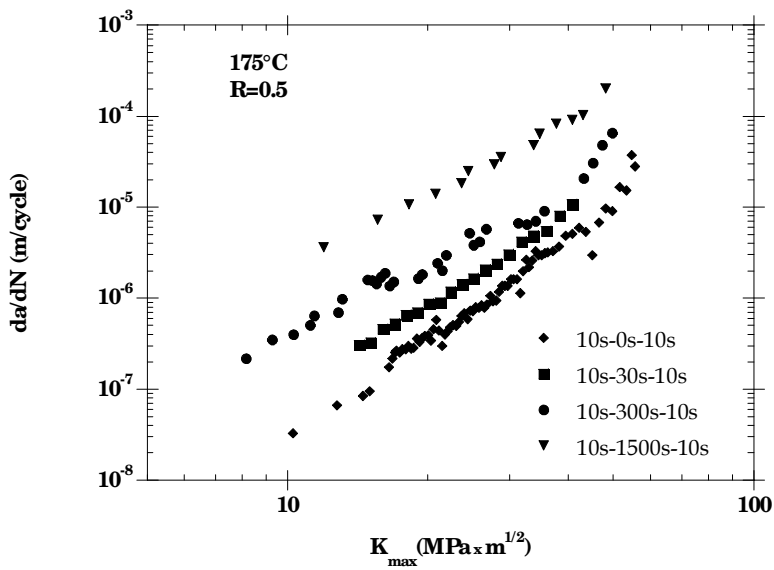


Fig. 10. Effect of the hold-time duration on the CFCG rates at 175°C in air.

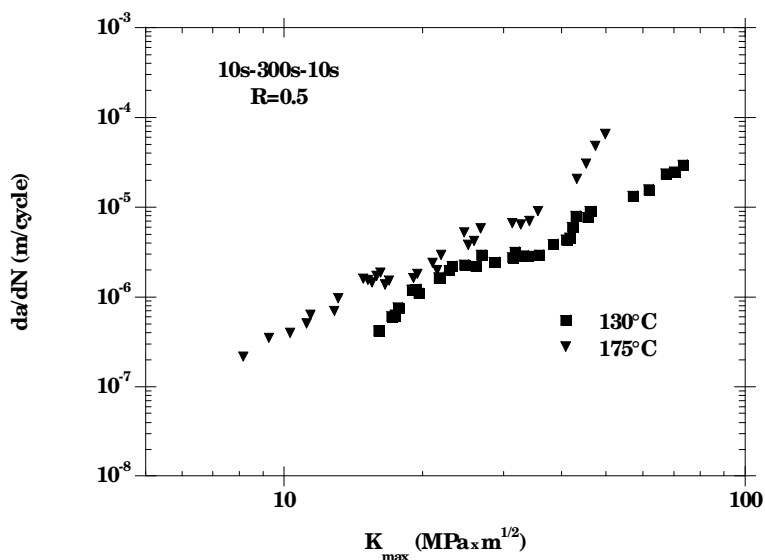


Fig. 11. Influence of temperature on CFCG rates for a 300s hold-time in air.

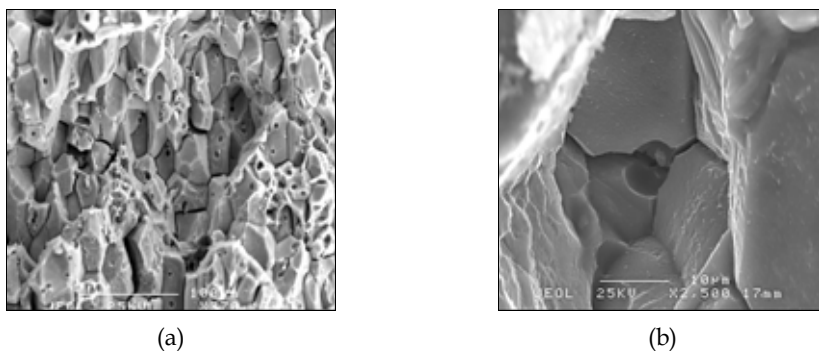


Fig. 12. CFCG fracture surfaces in air (a) intergranular decohesions ($K_{\max} = 23 \text{ MPa} \times \text{m}^{1/2}$, $da/dN = 2 \times 10^{-5} \text{ m/cycle}$, 10s-1500s-10s, 175°C); (b) cavitation at triple grain boundary ($K_{\max} = 30 \text{ MPa} \times \text{m}^{1/2}$, $da/dN = 2 \times 10^{-6} \text{ m/cycle}$, 10s-300s-10s, 175°C).

In order to analyse the observed crack growth enhancement quantitative measurements of the area fraction occupied by intergranular facets have been performed for different loading conditions (Hénaff et al., 2010). The results obtained under trapezoidal wave shape signals at 130°C and 175°C are presented in Figure 16 a and Figure 16 b, respectively, as a function of hold time. It can be noticed that, for a selected temperature, the longer the hold time, the higher the amount of intergranular facets, especially at low K values. Nevertheless, even for hold times as high as 3000s, the amount of intergranular facets never exceeds the amount obtained during CCG at the same K or K_{\max} value for a fixed temperature. Besides, for a given hold time value, the percentage of intergranular facets is higher at 175°C than at

130°C. Therefore a relationship between the amount of intergranular decohesions and the crack growth enhancement induced by creep damage with respect to fatigue at high frequency can be established.

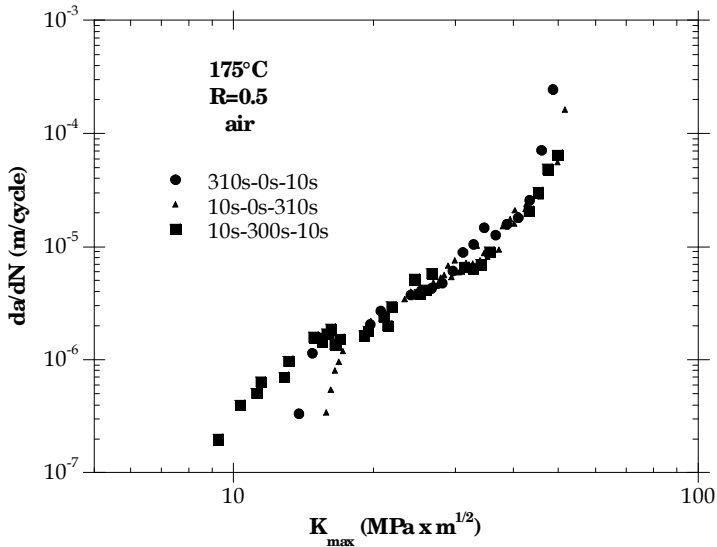
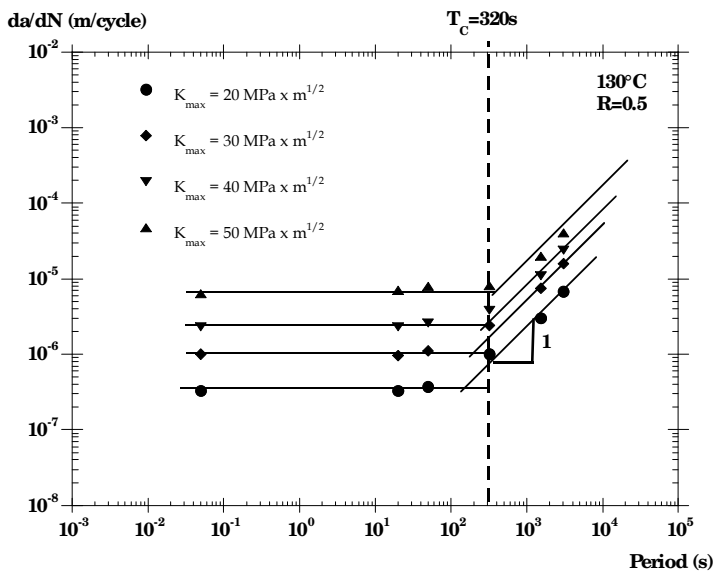
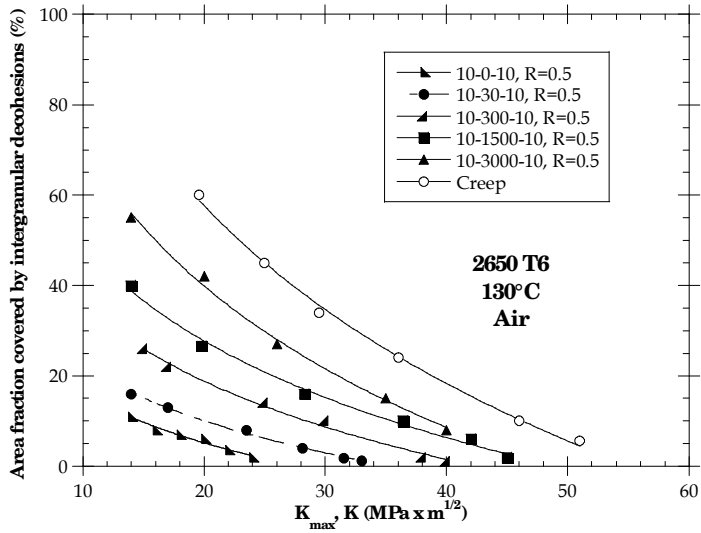


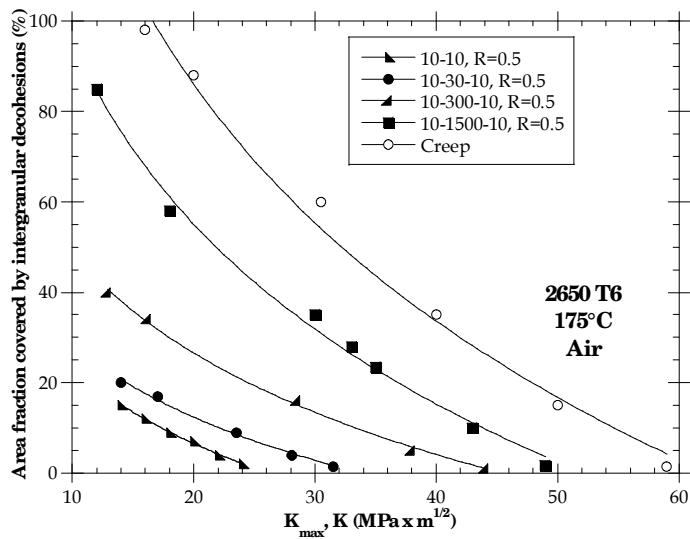
Fig. 13. CFCG rates for 3 different waveshapes of same period (320s) at 175°C in air.



(a)



(a)



(b)

Fig. 16. Percentage of area covered by intergranular decohesions as a function of maximum stress intensity factor for different loading cases (a) at 130°C; (b) at 175°C.

3.3 Influence of environment

The same experiments have been conducted in vacuum, mainly at 175°C, in order to evaluate the intensity of environmental effects on CGCG. With this respect, the results reported in Figure 17 indicate that, at high frequency (20Hz), FCGR in air are about fourfold higher than in vacuum. This enhancement can be mainly attributed to a surface adsorption effect (Hénaff et al., 1995), although the role of temperature on desorption may need to be more thoroughly analysed. However, while frequency has almost no influence on FCGRs in air at both temperatures as in vacuum at room temperature, a significant enhancement is observed at low frequency (0.05Hz) in vacuum at 175°C, suggesting that creep-fatigue effects may take place. The results of additional testing under creep-fatigue loading, typically trapezoidal load signals with hold time at the maximum load, are reported in Figure 18 using the same type of graph as in Figure 14. As observed in air, above a critical value of the period T_c , CFCG rates are proportional to the load period T . However, it should be noticed that the value of T_c determined in vacuum is lower than in air at the same temperature (Odemer, 2005). This might be accounted for by the enhanced FCGR in air as compared to vacuum which would induce a higher fatigue damage, so that a longer time is required to achieve higher cavitation-induced damage. Consistently, CCG and CFCG fracture modes in the 2650 alloy are characterised by a significant amount of intergranular decohesions induced by diffusion-controlled cavitation, regardless of environment as shown in Figure 15, for a trapezoidal 10s-300s-10s signal at 175°C. For a fixed K value it seems that the fraction of intergranular fracture is lower in air than in vacuum. This is confirmed by the quantitative measurements presented in Figure 19 which indicates that, for a selected K value, the percentage of fracture surface occupied by intergranular decohesions is higher in vacuum than in air. These observations suggest that the contribution of creep damage to the

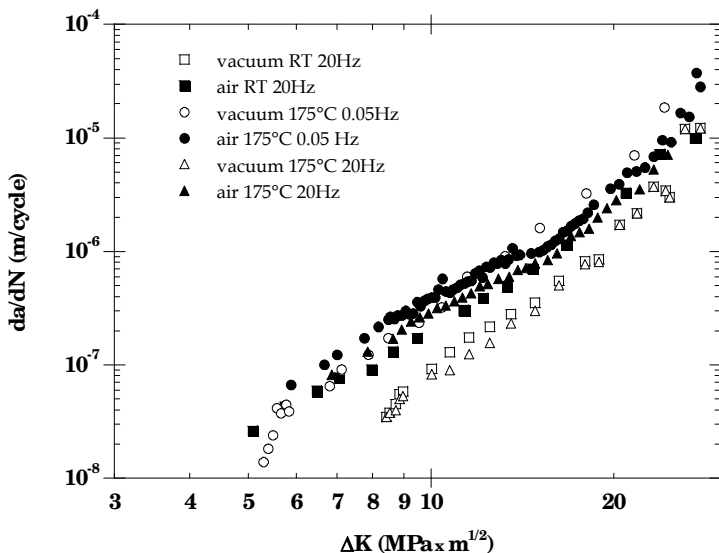


Fig. 17. FCG behaviour of the 2650 T6 alloy in air and in vacuum at 25°C and 175°C for two loading frequencies.

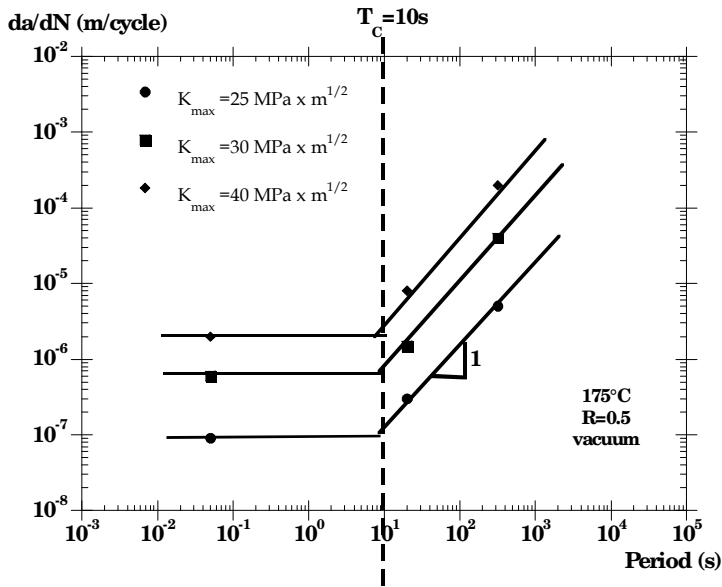


Fig. 18. CFCG rates as a function of the loading period for selected K_{max} values at 175°C in vacuum.

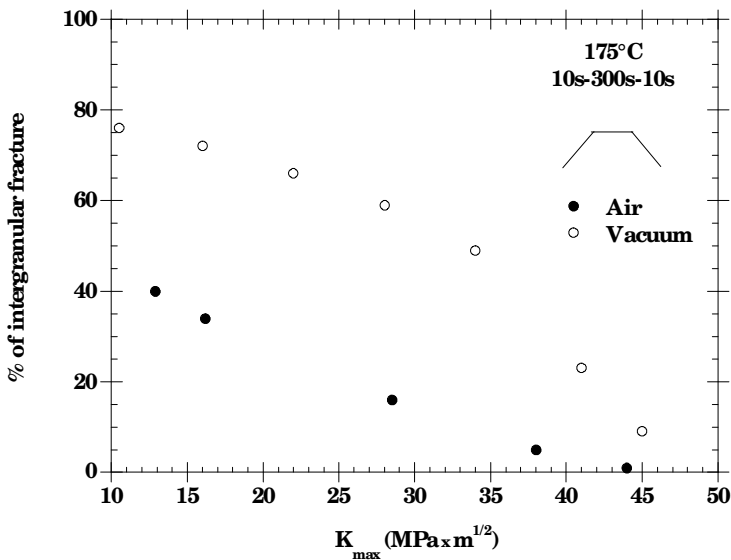


Fig. 19. Percentage of intergranular fracture mode during CFCG as a function of K_{max} in air and in vacuum at 175°C for a 10s-300s-10s trapezoidal signal.

total crack growth is lower in air than in inert environment for a fixed K_{\max} value, which consistent with CFCG rates results. They furthermore suggests that interactions between creep, fatigue and environmental exposure reduce the contribution of cavitation-induced intergranular fracture (Hénaff et al., 2007).

4. Predictions of Creep-fatigue Crack Growth Rates

The predictions of CFCGRs may be carried out using a simple cumulative rule. The basic assumption in such a case is that, for a fixed K value, the cyclic damage and the creep damage, each characterised by a crack growth increment, can be linearly added. Thus the crack growth increment per cycle is estimated as follows:

$$\left(\frac{da}{dN}\right)_{CFCG} = \left(\frac{da}{dN}\right)_{FCG} + T \times \left(\frac{da}{dt}\right)_{CCG} \quad (1)$$

where:

- T is the load period;
- $\left(\frac{da}{dN}\right)_{CFCG}$ represents the total crack growth rate in a creep-fatigue cycle;
- $\left(\frac{da}{dN}\right)_{FCG}$ denotes the crack growth rate induced by cyclic loading (typically under triangular waveform loading at high frequency) and determined by the ΔK value;
- $\left(\frac{da}{dt}\right)_{CCG}$ is the crack growth contribution due to creep and derived from the CCG curve

at the selected temperature using a value of K averaged over the cycle duration (for low frequency this average value is very close to K_{\max}).

The comparison between predictions and experimental data indicates that such a cumulative rule can correctly predict CFCGR in vacuum for the data available in most of the conditions investigated, namely in the 100°C-175°C and for K_{\max} values ranging between temperature range. An example of comparison is presented in Figure 20 a. However it should be noticed that the agreement observed at low ΔK is obtained by extrapolating the 4th power law dependence towards this low value. This suggests that the first domain observed at low K values on CCG curves and dependent on initial loading conditions might not be relevant in the CFCG conditions examined here.

The same prediction procedure has been applied to the crack growth behaviour in air. An example is presented in Figure 20 b. It can be seen that at low K values the predictions underestimates CFCGRs and overestimates at high K values. The results at low K values could also be improved by extrapolating the 4th power law to this regime. Anyway, the longer the hold-time, the larger the discrepancy between predictions and experimental results. An alternative procedure based on experimental observations is thus proposed in the following (Hénaff et al., 2008).

Figure 14 and Figure 18 clearly indicate that above a critical value of the load period T_c , CFCGRs are proportional to the load period, regardless of temperature and environment, suggesting that a Time-Dependent Crack Growth (TDCG) process takes place. In air however the results of cumulative damage rule predictions indicate that this TDCG process

might be different from the CCG process. On the basis of these observations, CFCG behaviour can be described using an empirical law accounting for cyclic and time-dependent damage and expressed as follows:

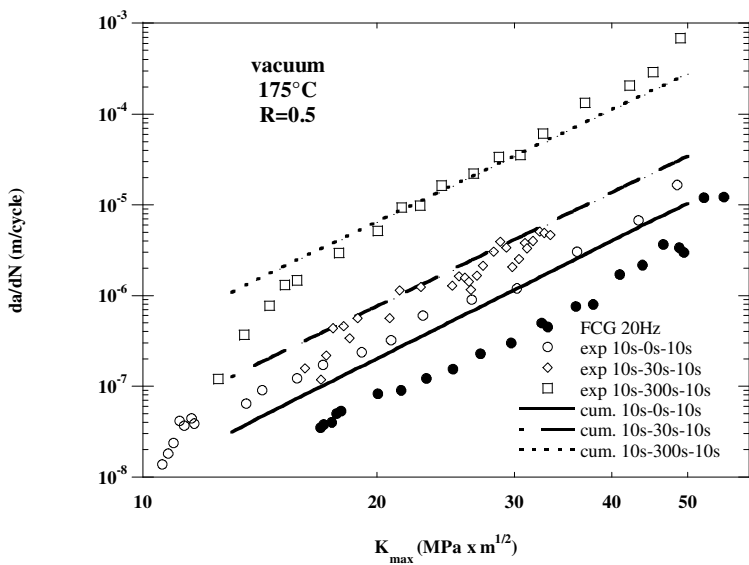
$$\left(\frac{da}{dN}\right)_{CFCG} = \left(\frac{da}{dN}\right)_{FCG} + (T - T_c) \times \left(\frac{da}{dt}\right)_{TDCG} \quad \text{for } T > T_c,$$

where $\left(\frac{da}{dN}\right)_{FCG}$ and $\left(\frac{da}{dt}\right)_{TDCG}$ denotes the fatigue crack growth and the time-dependent crack growth (TDCG) rate, respectively. A power-law of the same form than that used for CCG has been identified for the TDCG regime during CFCG. The values of the coefficient and exponent are identified using the data from right-hand side of the diagrams presented in Figure 14 and Figure 18, and compared to those identified for CCG. The values of the parameters for CCG and TDCG are compared in Table 3.

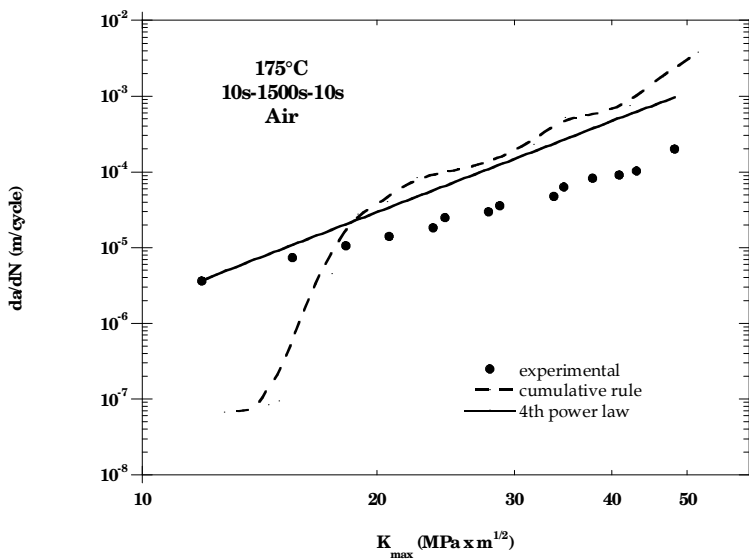
Environment	Temperature	Critical period T_c (s)	Time-dependent crack growth	
Air	175°C	50	TDCG	$\frac{da}{dt} = 1 \times 10^{-12} (K_{max})^{3.1}$
			CCG	$\frac{da}{dt} = 1.2 \times 10^{-13} (K_{max})^4$
Air	130°C	320	TDCG	$\frac{da}{dt} = 9.6 \times 10^{-12} (K_{max})^{1.8}$
			CCG	$\frac{da}{dt} = 4.0 \times 10^{-15} (K_{max})^4$
Vacuum	175°C	10	TDCG	$\frac{da}{dt} = 9.6 \times 10^{-14} (K_{max})^{4.1}$
			CCG	$\frac{da}{dt} = 9.8 \times 10^{-14} (K_{max})^{4.1}$

Table 3. Critical values of loading period, time dependent crack growth law and creep crack growth law as a function of environment and temperature.

The corresponding curves are compared for air and vacuum at 175°C in Figure 21 and in air at 130°C and 175°C and Figure 22. It can be seen that, while TDCG in vacuum is extremely close to the CCG law at 175°C, TDCG in air is slower than CCG and the K dependence is weaker ($n < 4$) than during CCG. This, in relation with the differences noticed in the fraction of intergranular facets (Figure 19) suggests that an interaction between fatigue damage, creep damage and environmental exposure takes place at the crack tip during propagation in air. This interaction would partly inhibit the cavitation process leading to intergranular fracture. The effect of this complex interaction is indeed beneficial at 175°C since TDCG is slower than CCG for a given K value, as shown in Figure 21, and therefore needs to be specifically determined. The situation at 130°C is perhaps more complex. The CCG curve in vacuum has not been determined at this temperature. However it can be considered that, as observed at 175°C, this curve is not basically modified by environment. Figure 22 indicates



(a)



(b)

Fig. 20. Comparison of experimental results and cumulative rule predictions at 175°C (a) in vacuum (b) in air.

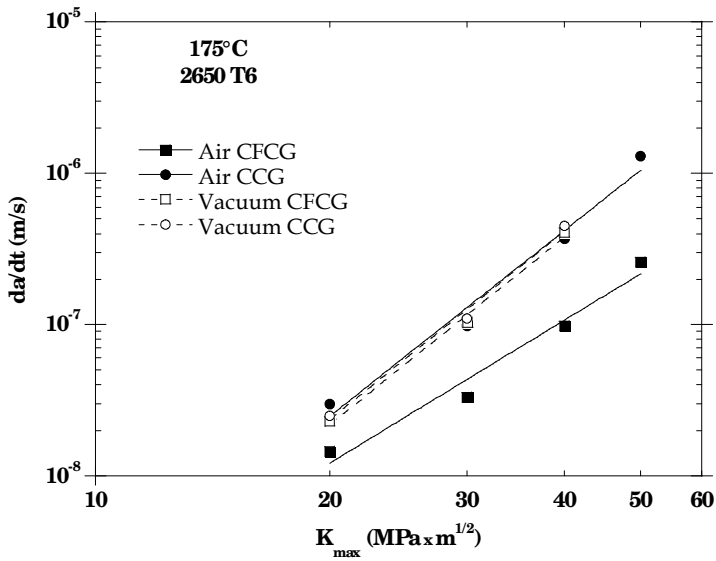


Fig. 21. TDCG and CCG behaviour of the 2650 T6 alloy in air and in vacuum at 175°C.

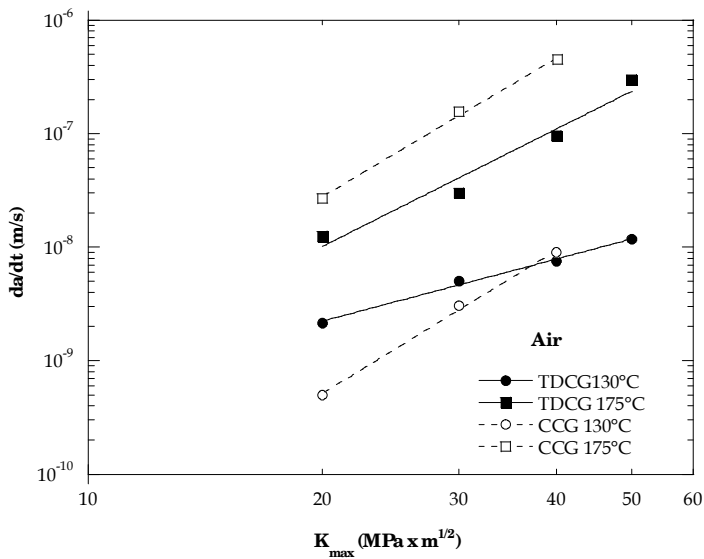


Fig. 22. TDCG and CCG behaviour in air at 130°C and 175°C.

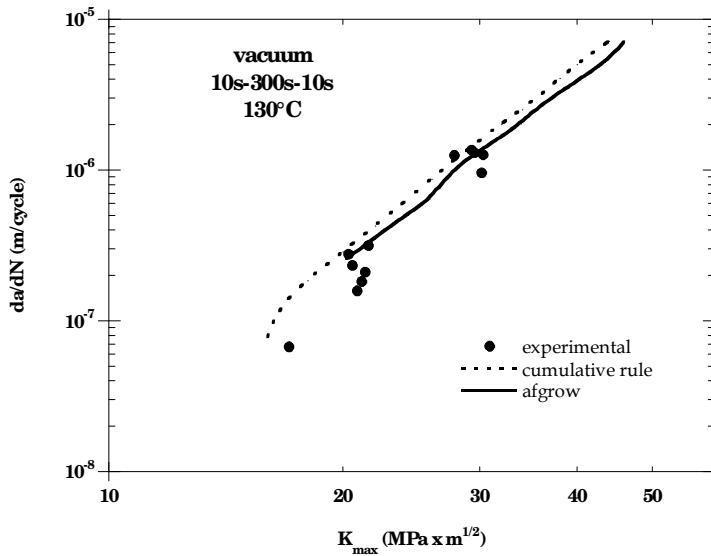


Fig. 23. Comparison of experimental data and predictions obtained using a cumulative damage rule and the time-dependent crack growth option of the AFGROW software for a 10s-300s-10s signal at 130°C in vacuum.

that the TDCG in air at low K_{\max} values is actually more rapid than CCG. This may indicate that at this temperature environment may rather promote the creep damage under CFCG. However the mechanisms responsible for this type of behaviour need clarification. Nevertheless the main interest of the approach proposed here is that the TDCG law could be identified for a fixed temperature at moderate values of frequency for selected values of stress intensity factor. This procedure would allow significant reductions in test duration and cost. In addition it can be easily implemented into software packages for crack growth predictions such as AFGROW (Harter, 2006). An example of calculation produced using the “time-dependent crack growth” option of AFGROW is compared in to experimental results and predictions obtained by the cumulative rule for a 10s-300s-10s trapezoidal signal in vacuum at 130°C. The CCG or the TDCG can be introduced in order to calculate crack growth life of more complex cracked structural elements. An assessment of the ability of this approach to account for the behaviour at extremely low but realistic frequency is however required. This point is under current investigation.

5. Summary and conclusions

In this chapter, the creep and creep-fatigue crack growth behaviour of a precipitation-hardened 2650 T6 aluminium alloy has been reviewed.

First, stable crack growth induced by creep has been characterised in the 100°C-175°C range. While temperature enhances creep crack growth rates in this range, this enhancement is particularly pronounced in the 130-160°C range and seems to saturate above 160°C. Creep crack growth is controlled by cavitation-induced intergranular fracture. Environment does not seem to affect CCG.

The fatigue crack growth behaviour at high frequency is almost unaffected by temperature in the range 25°C-175°C. However a deleterious influence of hold-time introduced at the maximum load and/or low frequency on crack growth rates under cyclic loading is observed in the 130°C-175°C temperature range in air and in vacuum. This effect is characterised by a significant contribution of intergranular fracture mode similar to that observed during creep crack growth under static loading. More precisely, above a critical value of loading period, crack growth rates are proportional to the loading period, regardless of the waveshape, indicating that a time-dependent crack growth process takes place. This time-dependent crack growth process seems to be affected by environment. Indeed in vacuum it corresponds with CCG, so that a cumulative rule of creep damage and fatigue damage provides realistic predictions. In air however the time-dependent crack growth process exhibits a K-dependence different from that observed during creep crack growth and dependent on temperature. As a consequence the cumulative rule using creep crack growth and fatigue crack growth data cannot account for the observed behaviour. An alternative procedure, based on a superposition model, is proposed to predict creep-fatigue crack growth rates at very low frequencies on the basis of results obtained at higher frequencies. This methodology could be used in standard crack growth life prediction methods but it has to be assessed by comparing predictions with experimental data obtained under very low frequency loadings. Finally this methodology could be extended to applications where aluminium alloys would be fatigued at elevated temperature and at low frequencies.

6. Acknowledgements

This work was carried out within the framework of the French National Programme on Supersonic Aircraft and the financial support by the French Ministry of Research is gratefully acknowledged.

7. References

- Bensussan, P., Jablonski, D. A. and Pelloux, R. M. (1984). A study of creep crack growth in 2219-T851 aluminum alloy using a computerized testing system. *Metallurgical and Materials Transactions a Physical Metallurgy and Materials Science*, Vol. 15A, No. January: 107-120.
- Bensussan, P., Maas, E., Pelloux, R. and Pineau, A. (1988). Creep crack initiation and propagation: fracture mechanics and local approach. *Journal of Pressure Vessel Technology*, Vol. 110, No. 1: 42-50.
- Ewing, D. J. F. (1978). Strip yield models of creep crack incubation and growth. *International Journal of Fracture*, Vol. 14, No. 1: 101-117.
- Harter, J. A. (2006). AFGROW USERS GUIDE AND TECHNICAL MANUAL (<http://www.siresearch.info>). WRIGHT-PATTERSON AIR FORCE BASE OH 45433-7542
- Hénaff, G., Marchal, K. and Petit, J. (1995). On fatigue crack propagation enhancement by a gaseous atmosphere: Experimental and theoretical aspects. *Acta Metall Mater*, Vol. 43, No. 8: 2931-2942.

- Hénaff, G., Menan, F. and Odemer, G. (2010). Influence of corrosion and creep on intergranular fatigue crack path in 2XXX aluminium alloys. *Engineering Fracture Mechanics*, Vol. 77, No. 11: 1975-1988.
- Hénaff, G., Odemer, G., Koffi, E., Benoit, G. and Journet, B. (2008). Prediction of creep fatigue crack growth rates in inert and active environments in an aluminium alloy, *Proceedings of International Conference on Fatigue Damage in Structural Materials VII*, Hyannis, MA, USA.
- Hénaff, G., Odemer, G. and Tonneau-Morel, A. (2007). Environmentally-assisted fatigue crack growth mechanisms in advanced materials for aerospace applications. *International Journal of Fatigue*, Vol. 29, No. 9-11: 1927-1940.
- Jata, K. V., Maxwell, D. and Nicholas, T. (1994). Influence of Environment and Creep on Fatigue-Crack Growth in a High-Temperature Aluminum-Alloy-8009. *Journal of Engineering Materials and Technology-Transactions of the Asme*, Vol. 116, No. 1: 45-53.
- Kaufman, J. C., Bogardus, K. O., Mauney, D. A. and Malcolm, R. C. (1976). Creep Cracking in 2219-T851 Plate at Elevated Temperatures. In: *Mechanics of Crack Growth, ASTM STP 590*, 149-168. American Society for Testing and Materials.
- Leng, Y. (1995). Study of creep crack growth in 2618 and 8009 aluminium alloys. *Metallurgical and Materials Transactions a Physical Metallurgy and Materials Science*, Vol. 26A, No.: 315-328.
- Majimel, J., Molenat, G., Casanove, M. J., Schuster, D., Denquin, A. and Lapasset, G. (2002). Investigation of the evolution of hardening precipitates during thermal exposure or creep of a 2650 aluminium alloy. *Scripta Materialia*, Vol. 46, No. 2: 113-119.
- Majimel, J., Molenat, G., Danoix, F., Blavette, D., Lapasset, G. and Casanove, M. J. (2002). A study of the hardening precipitation in a 2650 aluminium alloy for aeronautics. *Aluminium Alloys 2002: Their Physical and Mechanical Properties Pts 1-3*, Vol. 396-4, No.: 1025-1030.
- Menan, F. and Hénaff, G. (2009). Influence of frequency and exposure to a saline solution on the corrosion fatigue crack growth behavior of the aluminum alloy 2024. *International Journal of Fatigue, Fatigue Damage of Structural Materials VII*, Vol. 31, No. 11-12: 1684-1695.
- Menan, F. and Hénaff, G. (2009). Influence of frequency and waveform on corrosion fatigue crack propagation in the 2024-T351 aluminium alloy in the S-L orientation. *Materials Science and Engineering: A*, Vol. 519, No. 1-2: 70-76.
- Odemer, G. (2005). Tolérance au dommage avec prise en compte des interactions fatigue-fluage de l'alliage 2650-T6. PhD Thesis, *ENSMA*, Poitiers: 283
- Odemer, G., Hénaff, G. and Journet, B. (2006). Creep crack growth resistance of an age hardened aluminium alloy for supersonic applications. *Scripta Materialia*, Vol. 54, No. 1: 51-55.
- Odemer, G., Hénaff, G., Journet, B. and Rémy, L. (2006). Creep-fatigue interactions during crack growth in a 2650 T6 aluminium alloy, *Proceedings of Fatigue'2006, 9th International Congress on Fatigue*, Atlanta, Georgia, USA, Elsevier.
- Riedel, H. (1977). A Dugdale model for crack opening and crack growth under creep conditions. *Materials Science and Engineering*, Vol. 30, No. 3: 187-196.
- Sadananda, K. (1978). A Theoretical Model for Creep Crack-Growth. *Metallurgical Transactions a-Physical Metallurgy and Materials Science*, Vol. 9, No. may: 635-641.

Vitek, V. (1977). A theory of the initiation of creep crack growth. *International Journal of Fracture (Historical Archive)*, Vol. 13, No. 1: 39-50.

Vitek, V. (1978). A theory of diffusion controlled intergranular creep crack growth. *Acta Metallurgica*, Vol. 26, No. 9: 1345-1356.



Aluminium Alloys, Theory and Applications

Edited by Prof. Tibor Kvackaj

ISBN 978-953-307-244-9

Hard cover, 400 pages

Publisher InTech

Published online 04, February, 2011

Published in print edition February, 2011

The present book enhances in detail the scope and objective of various developmental activities of the aluminium alloys. A lot of research on aluminium alloys has been performed. Currently, the research efforts are connected to the relatively new methods and processes. We hope that people new to the aluminium alloys investigation will find this book to be of assistance for the industry and university fields enabling them to keep up-to-date with the latest developments in aluminium alloys research.

How to reference

In order to correctly reference this scholarly work, feel free to copy and paste the following:

Gilbert Hénaff, Grégory Odemer and Bertrand Journet (2011). Creep and Creep-Fatigue Crack Growth in Aluminium Alloys, Aluminium Alloys, Theory and Applications, Prof. Tibor Kvackaj (Ed.), ISBN: 978-953-307-244-9, InTech, Available from: <http://www.intechopen.com/books/aluminium-alloys-theory-and-applications/creep-and-creep-fatigue-crack-growth-in-aluminium-alloys>

INTECH

open science | open minds

InTech Europe

University Campus STeP Ri
Slavka Krautzeka 83/A
51000 Rijeka, Croatia
Phone: +385 (51) 770 447
Fax: +385 (51) 686 166
www.intechopen.com

InTech China

Unit 405, Office Block, Hotel Equatorial Shanghai
No.65, Yan An Road (West), Shanghai, 200040, China
中国上海市延安西路65号上海国际贵都大饭店办公楼405单元
Phone: +86-21-62489820
Fax: +86-21-62489821

© 2011 The Author(s). Licensee IntechOpen. This chapter is distributed under the terms of the [Creative Commons Attribution-NonCommercial-ShareAlike-3.0 License](#), which permits use, distribution and reproduction for non-commercial purposes, provided the original is properly cited and derivative works building on this content are distributed under the same license.